# Monitoring of scaling in dilute phase pneumatic conveying systems using non-intrusive acoustic sensors – A feasibility study

**Ingrid Bokn Haugland[1, 2, *], Jana Chladek[1] and Maths Halstensen[2]**

1. SINTEF Tel-Tek, SINTEF Industry, Kjølnes ring 30, N-3918 Porsgrunn, Norway

2. Faculty of Technology, Natural Sciences and Maritime Sciences, University of South-Eastern Norway, P.O Box 203 N-3901, Porsgrunn, Norway

*Advanced Powder Technology. 2019, 30*(8) 1634-1641.
DOI: https://doi.org/10.1016/j.apt.2019.05.012

# Monitoring of scaling in dilute phase pneumatic conveying systems using non-intrusive acoustic sensors – A feasibility study

**Ingrid Bokn Haugland[1, 2, *], Jana Chladek[1] and Maths Halstensen[2]**

1. SINTEF Tel-Tek, SINTEF Industry, Kjølnes ring 30, N-3918 Porsgrunn, Norway
2. Faculty of Technology, Natural Sciences and Maritime Sciences, University of South-Eastern Norway, P.O Box 203 N-3901, Porsgrunn, Norway

Corresponding author: Ingrid Bokn Haugland

Email: ingrid.haugland@sintef.no

Tel: +4790508941

Keywords: Scaling, depositions, adhesion, monitoring, PAT, pneumatic conveying

## Abstract

Scale formation in pneumatic conveying systems is a major industrial challenge. The underlaying scale formation mechanisms can be intricate as they often involve a combination of several mutually enhancing binding forces and can be affected by a number of different factors. A non-intrusive monitoring technique capable of measuring scale growth would be a valuable tool to investigate different scaling mechanisms. In this study, the feasibility of an active acoustic sensor technique for monitoring of scale growth in a pneumatic conveying system is evaluated. Tests are performed in a pilot scale pneumatic conveying system

transporting sand in dilute phase. The acoustic sensors conducts measurements on test pipes which are coated with a primer/powder mixture, one layer after the other, to simulate scale progression. Reference measurements of the coating layer thickness in the test pipes are obtained by a laser imaging technique for each added coating layer. A multivariate method is used to calibrate prediction models of the scale thickness using acoustic measurements as independent variables and the reference measurements as the dependent variable. Results show that the active monitoring method is capable of monitoring scale growth in pneumatic conveying systems and that dilute phase conveying of sand does not affect the precision of predictions made by the method.

## 1. Introduction

Depositions of unwanted material on the pipe walls in pneumatic conveying systems leads to substantial maintenance costs in some industries. Scale formation starts with deposition of particles on a clean surface, driven by particle-wall forces. Typically, the finest particles adhere to the roughest parts of the pipe wall [1]. Following this initial deposition, particle-particle forces become dominant as the thickness of the scale increases [2]. Particle-gas interactions are also influential in both these stages [2, 3]. In some cases, deposition layers keep growing until the pipeline is clogged, thus leading to system downtimes and loss of operational time. Aluminium production by the Hall-Héroult process is one example of an industrial application where scale formation is a significant challenge [4].

In order for a particle to adhere to the pipe wall, it has to travel from the bulk particle suspension towards the boundary layer region, be transported through the boundary layer and finally come in contact with the wall [5]. It will adhere to the wall if the sum of all the binding forces between the particle and the wall are larger than the sum of all forces pulling it away

from the wall [1]. Some of the main possible binding forces are solid bridges, liquid bridges, capillary forces, van der Waals' forces, chemical binding forces and electrostatic forces [1, 2, 5]. As many of these forces may be present simultaneously and have a mutually reinforcing effect [3], scale formation mechanisms can be intricate. The effect of parameters such as moisture, particle size [2] and temperature [1] further complicates the matter.

Even though scale formation in pneumatic conveying systems is a significant challenge for many industries, this field has not been paid much attention in previous research [2, 6]. The exception is adhesion driven by electrostatic forces, which has been studied extensively [2, 7], although the phenomenon is still not completely understood [2]. A monitoring method capable of measuring scale growth would be a useful tool for investigating scale formation. Such a method could be used to identify conditions favouring scale deposition and to investigate the effect of different influential parameters on scaling. Thus, a deeper understanding of the underlaying scale formation mechanism could be attained.

Initially defined for and implemented in the pharmaceutical industry, the process analytical technology (PAT) framework has been developed and spread to numerous different applications in recent years. PAT involves the use of advanced sensor technologies and data analysis techniques to monitor critical process parameters in order to attain better process understanding and control [8]. The measurement techniques are often indirect, requiring use of advanced data analysis methods to relate the measurements to the monitored parameters. Several such methods have been implemented in diverse powder handling processes, for instance to monitor solid mass flow in pneumatic conveying [9] or to characterize granular mixing [10]. However, no commercialized measurement equipment for monitoring of scaling in pneumatic conveying systems is currently available.

Acoustic chemometrics is a non-intrusive, real-time PAT methodology [11]. Passive acoustic chemometrics has been applied in several previous studies to monitor parameters in powder

handling processes. Monitoring of process state and product quality in a fluidized bed granulation process [12], end point detection in fluidized bed drying of biomass [13] and measuring of mass flow rate [14], material concentration [15] and material velocity [16] in dilute phase pneumatic conveying are some examples of applications. Also, particularly relevant for this study, the passive acoustic method has been used to monitor wax deposition thickness in oil production pipelines [17]. However, a limitation of the passive method is that it is sensitive to noise and vibrations created by a process. Active acoustic chemometrics, on the other hand, is expected to be more robust against such disturbances and should therefore be better suited to monitor scale formation in pneumatic conveying systems. The active method is a recently developed version of the acoustic technique, described in detail in [18], where the method was found to hold promise for monitoring of scaling in pipelines.

Acoustic chemometrics is dependent upon model calibration against reliable reference measurements of the monitored parameter. In a recent study, a laser imaging technique was developed for the purpose of obtaining reference measurements of scale growth in pipelines [19].

The study in [18] was conducted using a setup with single phase flow of air without particles and thus did not address the effect of powder transportation through pipelines on the performance of the active acoustic method. In the current study, experiments designed to test the robustness of the active acoustic method during dilute phase pneumatic conveying of sand were conducted.

## 2. Materials and methods

### 2.1. Pneumatic conveying rig

A pilot-scale pneumatic conveying rig situated in the powder research hall of SINTEF Tel-Tek (Porsgrunn, Norway) was used in the tests performed in this study. A schematic sketch of the test rig is shown in Fig. 1.

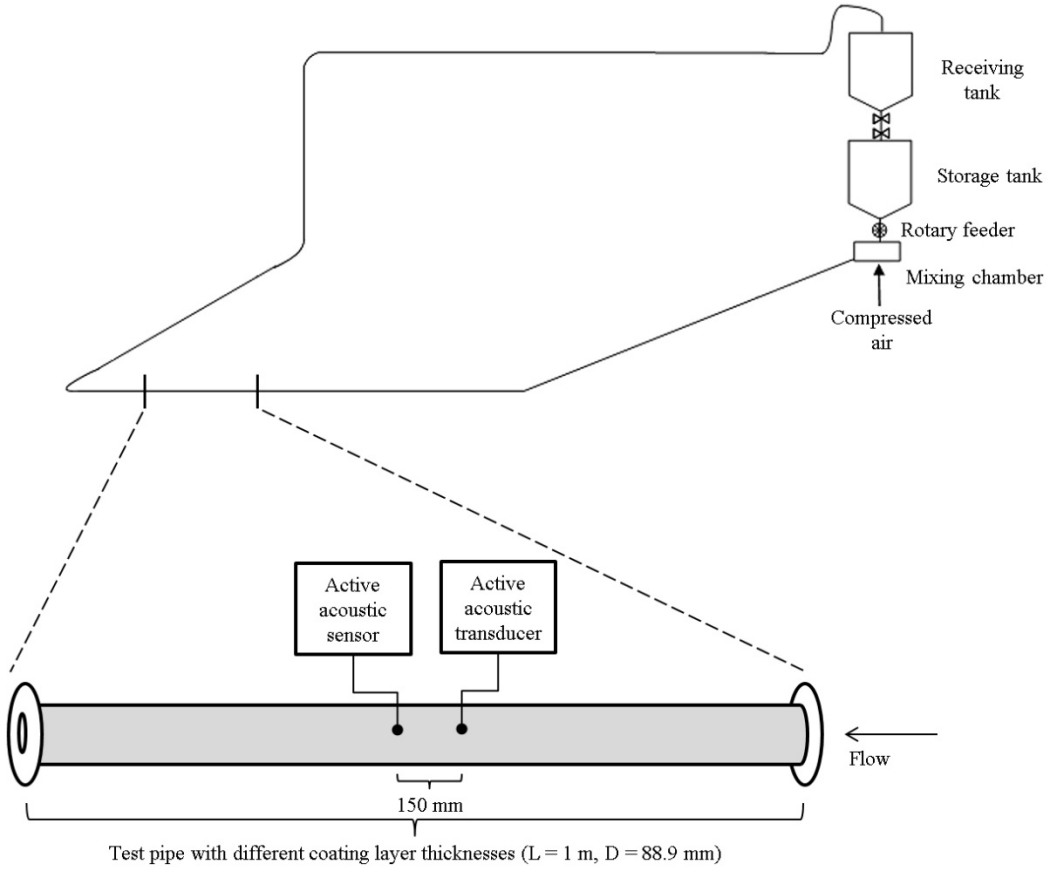


Figure 1: Schematic overview of the pneumatic conveying system and the test setup. Adapted from [20].

The main components of the pneumatic conveying system are a feeding tank, rotary feeder, mixing chamber, 3.5-inch stainless steel pipeline which has both vertical and horizontal sections as well as several bends, and a receiving tank at the end of the pipeline. As the material collected in the receiving tank can be transferred directly back into the feeding tank, the conveying system forms a closed loop. Transportation air is provided by a screw type air

compressor (Ingersoll Rand R110i) connected to an air dryer (Ingersoll Rand D1300IN-A). The air flow is controlled manually by a ball valve and is monitored by an air flow meter (Yokogawa, YF 108) installed close to the inlet of the pipeline. The material flow is controlled by setting the rotary feeding rate and the solid mass flow rate can be calculated based on measurements from three load cells on which the receiving tank is mounted. Eleven pressure transducers (General Electric, PTX5072-TC-A1-CA-H0-PA) installed along the pipeline are used to monitor the pressure drop.

In the experiments performed in this study, measurements where obtained from two test pipes using the active acoustic monitoring technique as well as the laser imaging technique mentioned above. The setup of the monitoring equipment can be seen in Fig. 1. An area following a long, straight section of the pipeline was selected as the test area in order to keep the flow conditions in the test pipes as stable as possible.

## 2.2. The test materials

In order to test the feasibility of the acoustic technique, it was important to attain steady and reproducible transportation conditions. A 50:50 wt % mix of two sand qualities was used as the conveying material, chosen for practical reasons as the mixture gave a stable flow. Some properties of the test materials are given in Table 1 [20].

Table 1: Overview of size distributions of test materials

| Sand quality | $x_{10}$ [mm] | $x_{50}$ [mm] | $x_{90}$ [mm] |
|---|---|---|---|
| 1 | 0.52 | 0.69 | 0.91 |
| 2 | 1.14 | 1.57 | 1.97 |

## 2.3. Active acoustic method

First presented in [18], the active acoustic method is a recently developed version of acoustic chemometrics. The measurement procedure of the active method consists of two main operations. A transducer sends an acoustic input signal into the monitored system and thus excites the system. Simultaneously, the frequency response of the signal is monitored by acoustic sensors. This output signal has been altered by the physical properties of the system which is monitored, and thus contains information about the system characteristics.

In this study, two piezo elements (one transducer and one sensor, Murata, 7BB-20-6L0) were attached to the test pipes in the setup shown in Fig. 1. Acoustic input signals (square waveforms with a constant amplitude and increasing frequencies spanning the interval 0-200 kHz) were created by a function generator (Escort EGC-3230) and sent into the system by the transducer. The output signals were measured by the sensor and amplified by a SAM-unit (applied chemometrics research group, University of South-Eastern Norway).

By means of a bandpass filter, unwanted frequencies were removed from the measured signals to reduce the impact of the aliasing effect during signal sampling in A/D conversion (sampling rate 400 kHz) by a DAQ unit (NI-Instruments). Subsequently, the output signals were transformed by a Blackman-Harris window function to avoid spectral leakage. Finally, the signals were converted from the time domain to the frequency domain by a Fast Fourier Transformation (FFT), producing acoustic spectra.

In the final step of the measurement procedure, chemometric methods, often referred to as multivariate data analysis, were used to extract information from the acoustic spectra. This is a crucial step as the acoustic method is indirect and requires calibration of models to relate the measurements to the monitored properties. A PC with customized LabVIEW-software (NI-

Instruments) was used to control the measurements and for the data acquisition. A more detailed description of acoustic chemometrics can be found in [11].

### 2.4. Laser imaging method

In order to calibrate models to relate the acoustic spectra to the coating thickness in a pipe, reliable reference measurements of the coating thickness are needed. In a previous study [19], a technique from [21] was further developed and a laser imaging device which can be used to obtain images of the coating layer inside a pipe was built for the purpose of obtaining such measurements.

The device consists of a rotating laser and a camera which are both attached to a mechanical support. When using the device to obtain reference measurements, the camera captures images with slow shutter speed while the laser illuminates a cross section of the inner wall of a pipe. This produces images of traces of laser light illuminating the pipe cross section. Subsequently, the captured images are processed to isolate the laser traces. Calculations of the coating layer thickness are performed based on the processed images using a MATLAB-code (version 9.1.0.441655, R2016b). The laser imaging method is described in detail in [19].

### 2.5. Comparison of measurement methods

Acoustic chemometrics is a non-intrusive method which can be used for online monitoring of many different process parameters. Installation of the measurement equipment is relatively straightforward. "Clamp on" sensors can be mounted directly to the process equipment in the selected test area; a test pipe in a pneumatic conveying system in this study. The laser method, on the other hand, is invasive and less practical to use. Measurements can only be obtained

during downtime of the pneumatic conveying system. Every time a measurement is going to be made, the test pipe must be detached from the pipe system. Thus, the laser imaging technique is not well suited for continuous monitoring of scale growth in a pipe, but still works well as a reference technique since it is sufficient to collect reference measurements at a lower sampling frequency.

In [18], an error called the root mean square error of prediction (RMSEP) was calculated for different prediction models of scale thickness in a pipe calibrated from acoustic spectra. The prediction error (RMSEP) of the best model was 0.431 mm. The accuracy and reproducibility of the laser imaging method were tested in [19]. For 10 different imitated deposition layer thicknesses, values estimated by the technique were compared by "true values" measured by a Vernier caliper. By this manner, the uncertainty of the method was found to be below 0.1 %, corresponding to around 0.1 mm. Accordingly, the laser imaging method is the most reliable of the two techniques. The study in [19] was conducted in a rather ideal environment; the uncertainty of the laser imaging method is expected to be somewhat higher for more complex scale structures. However, as the coating layers which were added to the test pipes in this study were relatively even and with smooth surfaces, the test conditions of this study were similar to the test conditions in [19]. Thus, it can be assumed that in the study presented in this paper the uncertainty of the laser imaging method will be of the same level as in [19].

The acoustic measurements are affected by and represents some area along the test pipe of at least 10-15 cm. Thus far, the total reach of the method has not been systematically investigated. In contrast, the laser imaging method is a point measurement, giving information about a cross section of the test pipe only. However, the latter method can give information about the spatial distribution of scale within this cross section, which the acoustic technique cannot provide. This feature is not important in the current study, but for an industrial

application where more complex structures and shapes of depositions can be expected, such information could be of considerable value.

In comparison to comparable measurement techniques, both the acoustic method and the laser imaging method are relatively inexpensive.

## 2.6. Multivariate data analysis

Datasets containing measurements of several variables for the same set of objects can be referred to as multivariate data. Multivariate data analysis involves simultaneous investigation of the variables contained in such datasets [22]. In general, the field comprises of various methods and procedures for retrieving information from multivariate data.

Partial least squares regression (PLS-R) is one such method which can be used for investigating the relationship between data collected in a matrix **X** and in a vector **y** [22]. The variables in **X** are typically easy to monitor and contain underlying information about **y**, which in contrast is difficult, expensive and/or time consuming to measure. In this situation, the ultimate goal of PLS-R is to find a way to predict values of **y** based on measurements of **X**. Thus, indirect measurements of **y** can be obtained by monitoring **X**, making a convenient way to monitor **y** available.

The relationship between **X** and **y** can be established by calibrating a model using the columns in **X** as the independent variables and **y** as the dependent variable, also referred to as the response. PLS-R creates such models using an algorithm which summarizes all the information in **X** which is relevant to model **y** in a few components. The model is built from these components, thus reducing the noise in the model by leaving out variations in **X** which is not relevant for **y**. Additionally, the data analysis is drastically simplified as only a few components need to be investigated.

In order to calibrate models, a calibration dataset containing measured values of **X** and corresponding values of **y** is needed. Once a model has been calibrated, it must be validated to check whether it is able to make reliable predictions of future values of **y** based on future measurements of **X**. Test set validation uses a new, independent dataset obtained in a similar manner as the calibration set for this purpose. To check the predictive ability of the model, a prediction error (RMSEP) can be calculated. This is done by comparing values of **y** predicted by the model using the **X** in the validation set as input and the reference value of **y** contained in the validation set, as described in Eq. 1. In Eq. 1, n is the number of measurements in the validation set. Additionally, a scatter plot of the predicted and measured values of **y** are typically inspected [23]. Some statistics derived from this plot can also be used when evaluating the model; the slope, offset and squared correlation coefficient of a linear curve fitted to the points in the plot.

$$\mathrm{RMSEP} = \sqrt{\frac{\sum_{i=1}^{n}\left(\hat{y}_{i,\mathrm{predicted}} - y_{i,\mathrm{reference}}\right)^2}{n}} \quad (1)$$

Model validation is also used to evaluate how many components should be included in the model. One way to decide on the number of components to use is to find the first minimum value in a residual validation variance plot. It is also helpful to consider t-u plots, depicting the "inner relationship" between **X** and **y**, when making this assessment [24]. Additionally, such plots are used to check if there are any deviating points, typically referred to as outliers, in the data [23].

The data analysis in this study was performed using Unscrambler version 10:3 (Camo software AS, Oslo, Norway).

2.7. Test procedure

In this study, two equivalent sets of experiments were performed to produce a calibration set and validation set, respectively. Separate test pipes were used when obtaining each of the two experimental sets. When installing the measurement equipment to the test pipes, efforts were made to make them as similar as possible to minimize the differences in the measurement sets induced by variations in the installation.

During the experiments, sand was conveyed through the test rig (Fig. 1) using pre-set values for air flow rate and solid feeding rate. These values were selected based on initial tests performed to determine suitable transportation conditions giving a stable dilute phase flow. Measurements were conducted when the pneumatic conveying system had reached the selected air flow and solid feeding rates and was in steady state. An overview of the test conditions can be seen in Table 2.

Table 2: Overview of test conditions

| Inlet air flow rate [$Nm^3/h$] | Air temperature [° C] | Solid mass flow rate [kg/s] | Solid loading ratio | Reynolds number |
|---|---|---|---|---|
| 300 | 15 | 0.26 | 1.3 | $1.8*10^5$ |

Each of the sets of experiments was initiated by obtaining measurements from the test pipes in their current states. Subsequently, the test pipes were coated with even layers of a 9:1wt % mixture of epoxy primer and alumina powder using a rotation rig described in detail in [25]. The coating mixture was intended to resemble scale depositions in the pipes. One layer after another was added to each of the test pipes, and measurements were obtained for every new layer. In each experiment, three replicate measurements where obtained by the active acoustic

method. Additionally, three images were captured from each side of the pipe using the laser device. The test pipes had to be detached from the main conveying rig every time a coating layer was added and subsequently reattached to the rig to conduct the measurements. In total, 12 layers of the coating mixture was added to each test pipe.

The resulting calibration and validation sets consisted of measurements obtained by the acoustic monitoring method for the initially clean test pipes and for every added coating layer. Additionally, corresponding values for the total thickness of coating after each new layer had been added, were calculated from the laser device images. The variables in the dataset were mean centred and scaled to unit variance. PLS-models were calibrated based on the data using the acoustic measurements as independent variables **X** and the calculated coating layer thicknesses as the dependent variable **y**, also called the response.

## 3. Results and discussion

### 3.1: Reference measurements by laser imaging method

Fig. 2 shows some examples of raw images obtained by the laser device together with the pre-processed versions of the images. The raw images were obtained from the inside of one of the test pipes used in this study. Fig. 2 a) represents the clean test pipe before any coating layers had been added and Fig. 2 c) were obtained from the test pipe after it had been coated with 12 layers of the coating mixture. Fig. 2 b) and Fig. 2 d) shows the corresponding pre-treated images. The white circles in the images in Fig. 2 were created from the laser light tracing the inner wall of a cross-section of the test pipe. In the pre-processed versions of the images, the circular laser traces have been isolated. As can be seen from the images in Fig. 2, the diameter of the laser light circle decreases as the coating layer thickness in the pipe increases.

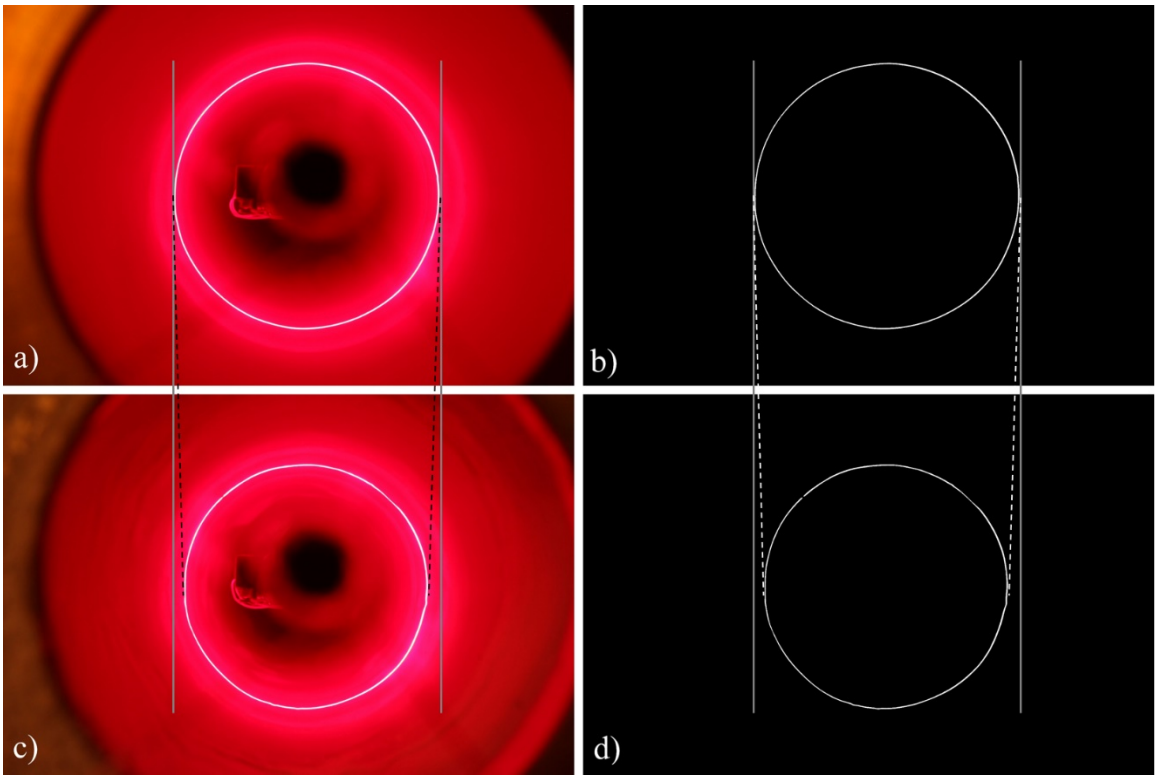


Figure 2: Raw images (a) layer 0 (clean pipe) and c) layer 12) obtained by the laser device and their respective pre-treated versions (b) layer 0 (clean pipe) and d) layer 12).

The pre-processed images were used to calculate the total coating thickness in the test pipes after the addition of each new coating layer. A MATLAB code was applied to perform the calculations. The resulting layer thicknesses are listed in Table 3, in which each figure is an average of the calculated values from six images, three from each side of the test pipes.

Table 3: Overview of estimated total thicknesses [mm] after adding each new coating layer to the two test pipes.

| | Calibration set Thickness [mm] | Validation set Thickness [mm] |
|---|---|---|
| Layer 0 | 0 | 0 |
| Layer 1 | 0.43 | 0.26 |
| Layer 2 | 0.65 | 0.50 |
| Layer 3 | 0.95 | 0.80 |
| Layer 4 | 1.24 | 1.03 |
| Layer 5 | 1.53 | 1.28 |
| Layer 6 | 1.83 | 1.59 |
| Layer 7 | 2.31 | 1.88 |
| Layer 8 | 2.51 | 2.24 |
| Layer 9 | 2.84 | 2.46 |
| Layer 10 | 3.10 | 2.71 |
| Layer 11 | 3.55 | 2.95 |
| Layer 12 | 3.85 | 3.01 |

As can be seen in Table 1, the total coating thickness after adding each of the layers is deviating in the two test pipes. However, this does not affect the calibration of models based on the data as it is not necessary to have similar response values in the calibration and validation sets in PLS-R. The main requirement for successful model calibration in this case is the availability of precise measurements of the thicknesses of each layer, which the laser imaging method provides. Also, it is important that the data in the validation set is within the

range where the calibrated model is valid. Thus, the test pipe with the thickest total coating layer was used as the calibration set.

### 3.2. Initial PLS-R modelling results

A PLS-R model was calibrated using the acoustic spectra as the independent variables and the values in Table 3 as the dependent variable. An overview of the PLS-R calibration results can be seen in Fig. 3. Based on inspection of the Residual Validation Variance plot in Fig. 3, it was decided to include two components in the model. The Predicted vs. Reference plot and the model statistics show that the model can give fairly good predictions of new values of the response based on new measured acoustic spectra. This assessment is supported by inspection of the Predicted and Reference plot, although the plot also reveals that some of the total coating layer thicknesses are considerably overpredicted or underpredicted by the model. Inspection of the X-y Relation Outlier plot reveals that no outliers are present in the data. Furthermore, the locations of the points in the X-y Relation Outlier plot suggest that the data has a non-linear structure. This is most likely a result of a non-linear decrease in the acoustic response as the total coating layer increases. As PLS-R models are linear, they are not well suited to describe non-linear data. Thus, efforts were made to linearize the data in order to enable calibration of reliable models by PLS-R.

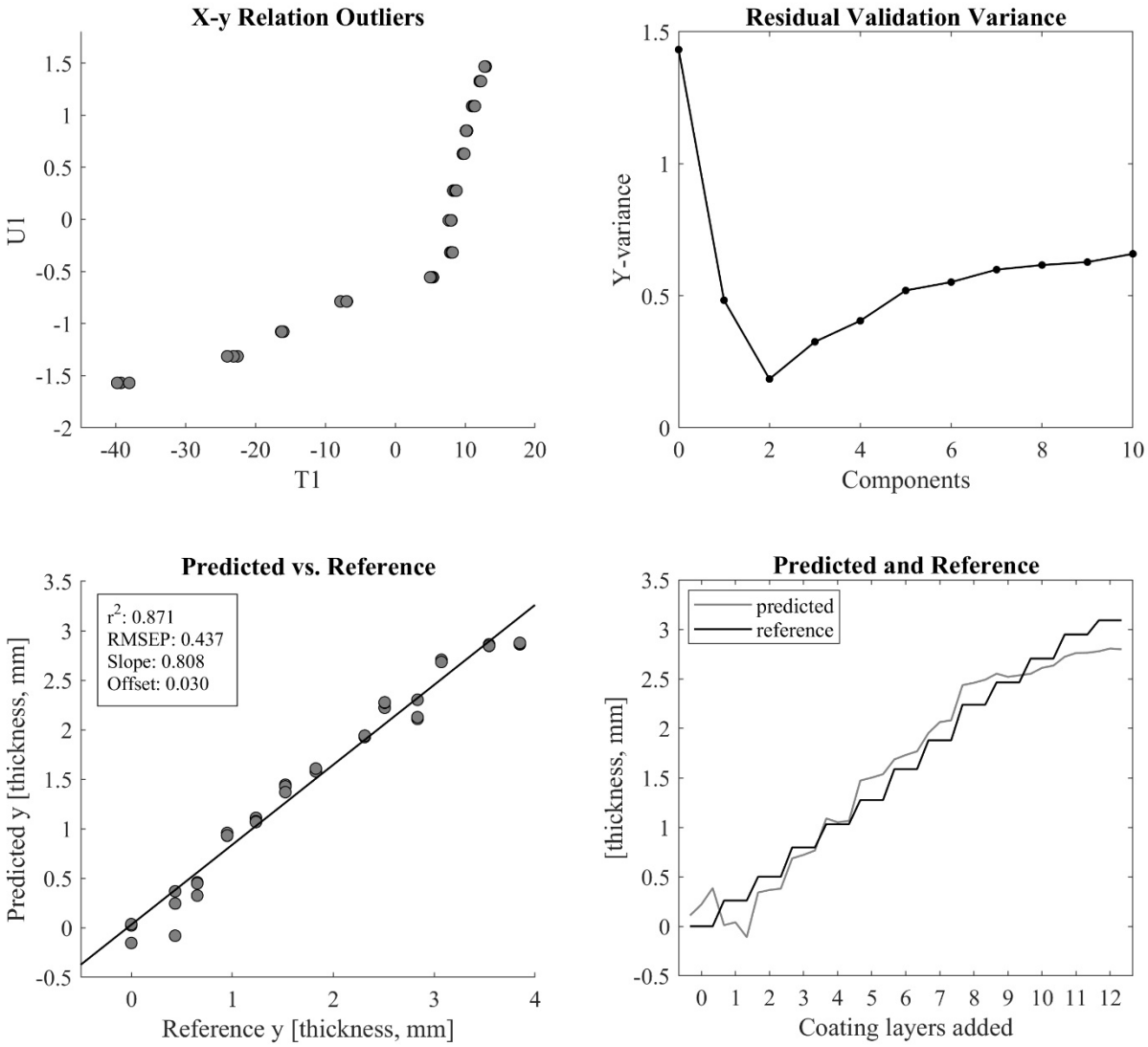


Figure 3: Initial PLS-R calibration results.

### 3.3. Final PLS-R modelling results

The data in the **X** matrix in the calibration and validation datasets were linearized by a logarithmic transformation. Fig. 4 shows the PLS-R calibration results from a model calibrated from the linearized data. The Residual Validation Variance plot in Fig. 4 suggest that three components should be included in the model. The inclusion of an additional component in comparison to the previous model is a result of the data transformation. As can be seen from the X-y Relation Outliers plot in Fig. 4, some of the non-linear structure is

persisting in the data. However, the new model represents a significant improvement in comparison with the initial model. As can be seen in the Predicted vs. Reference plot, model statistics and the Predicted and Reference plot, the new model succeeds in predicting new response values with a good precision. Thus, as the model performed sufficiently at this point and as excessive alteration of the raw data is unadvisable, additional transformations to further linearize the data was deemed unnecessary.

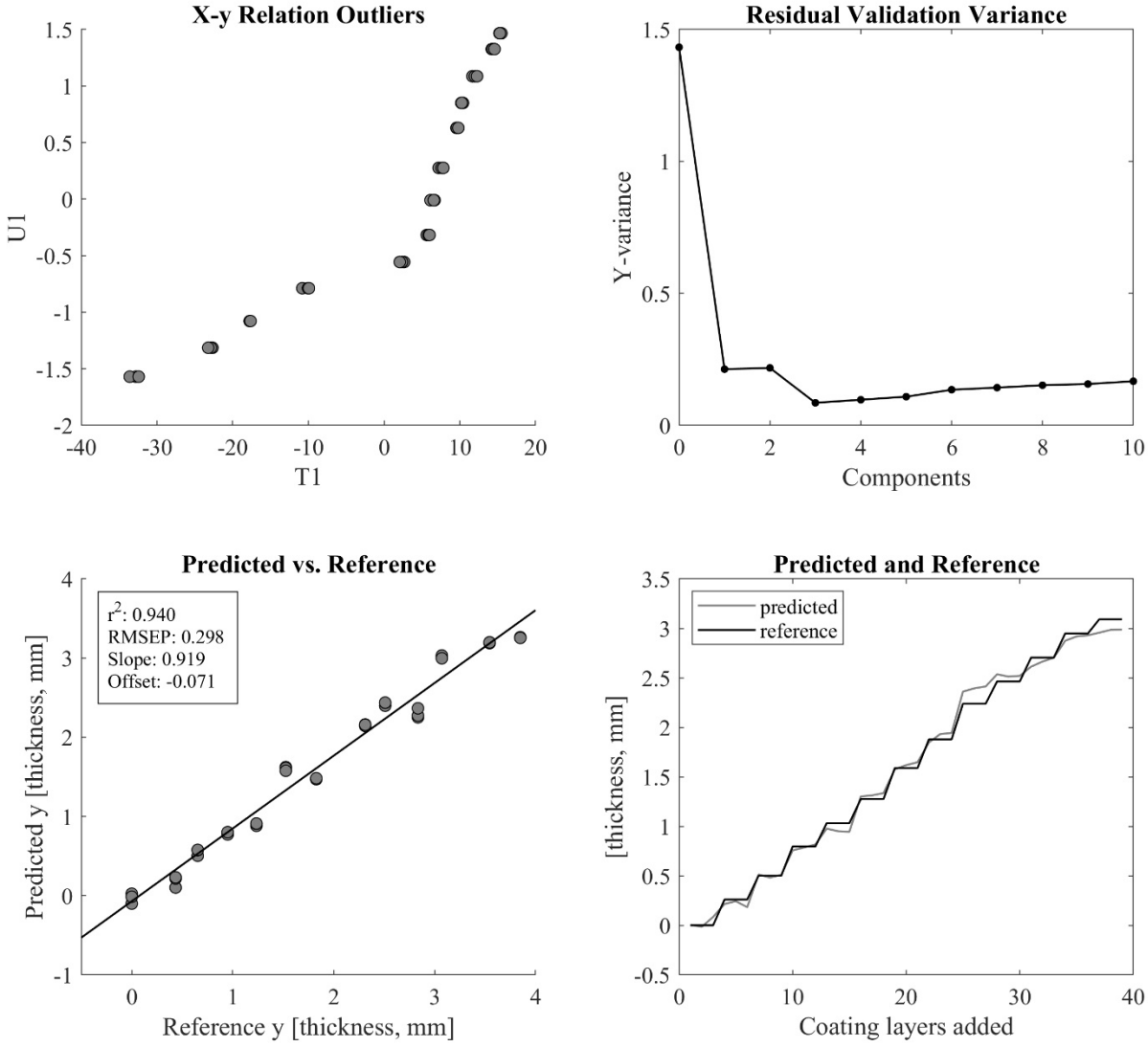


Figure 4: PLS-R calibration results after linearization of **X**-matrix.

3.4. Comparison with previous work

The model statistics from the models calibrated in this study are compared with the corresponding model statistics from the previous study [18] in Table 4.

Table 4: Comparison of model statistics of models calibrated in this study and the corresponding results from the previous study

| Model | # components | Offset | Slope | RMSEP (mm) | $r^2$ |
|---|---|---|---|---|---|
| Previous study | 2 | -0.055 | 0.827 | 0.431 | 0.834 |
| Current study, initial model | 2 | 0.030 | 0.871 | 0.437 | 0.871 |
| Current study, final model | 3 | -0.071 | 0.919 | 0.298 | 0.940 |

From Table 4, it can be seen that the initial model calibrated in this study gave an equivalent performance as the model from the previous study [18] which was performed with single-phase flow of air without particles. An important implication of this finding is that the performance of the active acoustic method is not influenced by dilute-phase conveying of powder through the test pipes. Thus, the method is robust against influence from fluctuations and noise generated by the monitored system. Although the X-y Relation Outlier plot in the previous study [18] suggested that the data was non-linear, the data was not linearized in that study. As can be seen from Table 4, the model statistics of the final model are considerably better than the other models. Accordingly, model performance can be significantly improved by linearizing the data.

## 4. Conclusion

In this study, the feasibility of monitoring scale growth in a test pipe using an active acoustic method during dilute phase conveying of sand was investigated. It was found that the method is capable of providing good predictions of scale thickness. Reliable reference measurements of scale growth in the test pipes were obtained by the laser imaging method. Comparison with the findings from the previous study indicated that the predictive ability of the active acoustic method is unaffected by dilute phase pneumatic conveying. Furthermore, it was found that a logarithmic transformation of the acoustic spectra diminishes the non-linear structure of the data and thus leads to a significant improvement in the performance of models calibrated from the acoustic measurements.


## Acknowledgements

The authors would like to thank Hydro Aluminium AS, GE Power Norway AS, Omya Hustadmarmor AS and the Norwegian Research Council for financial support of this project (project no. 247789).


## Nomenclature

| | |
|---|---|
| Calibration set | Dataset containing measurements of **X** and corresponding measurements of **y**, used to calibrate models |
| n | Number of rows in **X** and **y** in the validation set |
| Offset | Offset of the regression curve in a predicted vs. measured plot |
| Outlier | Deviating measurement |
| PAT | Process analytical technology |

| | |
|---|---|
| PLS-R | Partial least squares regression |
| $r^2$ | Squared correlation coefficient |
| RMSEP | Root mean square error of prediction |
| Slope | Slope of the regression curve in a predicted vs. measured plot |
| Validation set | Dataset containing measurements of **X** and corresponding measurements of **y**, used to validate models |
| **X** | Multivariate data matrix, independent variables in calibration |
| **y** | Response variable, dependent variable in calibration |
| $\hat{\mathbf{y}}$ | Estimator of **y** |

## References


[1] W.B. Pietsch, Adhesion and Agglomeration of Solids During Storage, Flow and Handling - A Survey, Journal of Engineering for Industry, 91 (1969) 435-448.

[2] G.E. Klinzing, Gas-solid transport, McGraw-Hill, New York, 1981.

[3] M.M. Awad, Fouling of heat transfer surfaces, in: A. Belmiloudi (Ed), Heat Transfer-Theoretical Analysis, Experimental Investigations and Industrial Systems, InTech, 2011, pp. 505-542.

[4] N.R. Dando, S.J. Lindsay, Hard Gray Scale, in: G. Bearne, M. Dupuis, G. Tarcy (Eds.), Essential Readings in Light Metals, Aluminium Reduction Technology, Wiley, Hoboken, 2013, pp. 602-607.

[5] P.R. Rennie, X.D. Chen, A.R. Mackereth, Adhesion characteristics of whole milk powder to a stainless steel surface, Powder Technology, 97 (1998) 191-199.

[6] R.J. Reuvekamp, M.B. Ray, A.C. Hoffmann, Deposition of a fine powder in horizontal pipelines and bends, Chemical Engineering Communications, 189 (2002) 849-864.

[7] F.J. Wang, J.X. Zhu, J.M. Beeckmans, Pressure gradient and particle adhesion in the pneumatic transport of cohesive fine powders, International Journal of Multiphase Flow, 26 (2000) 245-265.

[8] L.L. Simon, H. Pataki, G. Marosi, F. Meemken, K. Hungerbühler, A. Baiker, S. Tummala, B. Glennon, M. Kuentz, G. Steele, H.J.M. Kramer, J.W. Rydzak, Z. Chen, J. Morris, F. Kjell, R. Singh, R. Gani, K.V. Gernaey, M. Louhi-Kultanen, J. O'Reilly, N. Sandler, O. Antikainen, J. Yliruusi, P. Frohberg, J. Ulrich, R.D. Braatz, T. Leyssens, M. von Stosch, R. Oliveira, R.B.H. Tan, H. Wu, M. Khan, D. O'Grady, A. Pandey, R. Westra, E. Delle-Case, D. Pape, D. Angelosante, Y. Maret, O. Steiger, M. Lenner, K. Abbou-Oucherif, Z.K. Nagy, J.D. Litster, V.K. Kamaraju, M.-S. Chiu, Assessment of Recent Process Analytical Technology (PAT) Trends: A Multiauthor Review, Organic Process Research & Development, 19 (2015) 3-62.

[9] Y. Zheng, Q. Liu, Review of techniques for the mass flow rate measurements of pneumatically conveyed solids, Measurement, 44 (2011) 589-604.

[10] H. Nadeem, T.J. Heindel, Review of noninvasive methods to characterize granular mixing, Powder Technology, 332 (2018) 331-350.

[11] M. Halstensen, K.H. Esbensen, Acoustic chemometric monitoring of industrial production processes, in: K.A. Bakeev (Ed.), Process Analytical Technology, 2nd ed., Wiley-Blackwell, 2010, Oxford, 2010, pp. s. 281-302.

[12] M. Halstensen, P. de Bakker, K.H. Esbensen, Acoustic chemometric monitoring of an industrial granulation production process—a PAT feasibility study, Chemometrics and Intelligent Laboratory Systems, 84 (2006) 88-97.

[13] F.N. Ihunegbo, C. Ratnayake, M. Halstensen, Acoustic chemometrics for on-line monitoring and end-point determination of fluidised bed drying, Powder Technology, 247 (2013) 69-75.

[14] K.H. Esbensen, M. Halstensen, T. Tønnesen Lied, S. Arild, J. Svalestuen, S. de Silva, B. Hope, Acoustic chemometrics—from noise to information, Chemometrics and Intelligent Laboratory Systems, 44 (1998) 61-76.

[15] C. Wagner, F.N. Ihunegbo, M. Halstensen, K.H. Esbensen, Acoustic chemometrics for material composition quantification in pneumatic conveying — The critical role of representative reference sampling, Powder Technology, 237 (2013) 506-513.

[16] M. Halstensen, F.N. Ihunegbo, C. Ratnayake, K. Sveinsvold, Online acoustic chemometric monitoring of fish feed pellet velocity in a pneumatic conveying system, Powder Technology, 263 (2014) 104-111.

[17] M. Halstensen, B.K. Arvoh, L. Amundsen, R. Hoffmann, Online estimation of wax deposition thickness in single-phase sub-sea pipelines based on acoustic chemometrics: A feasibility study, Fuel, 105 (2013) 718-727.

[18] I.B. Haugland, M. Halstensen, Online Acoustic Chemometrics Monitoring of Scale Deposition Thickness in Pneumatic Conveying Systems: A Feasibility Study, in: Proc. 5th International Symposium of Reliable Flow of Particulate Solids (RELPOWFLO), Skien, Norway, 2017.

[19] I.B. Haugland, M. Halstensen, A Technique for Obtaining Reference Measurements to Calibrate Deposition Models for Pipelines, Chemical Engineering & Technology, (2018).

[20] A. Malagalage, Pneumatic conveying and storage of wet particles to illustrate offshore drill cutting handling, Ph.D. Thesis, University of South-Eastern Norway, 2018.

[21] R. Hoffmann, L. Amundsen, Single-Phase Wax Deposition Experiments, Energy & Fuels, 24 (2010) 1069-1080.

[22] H. Martens, T. Næs, Multivariate calibration, Wiley, Chichester, 1989.

[23] K.H. Esbensen, Multivariate data analysis - in practice : an introduction to multivariate data analysis and experimental design, 5th ed., Camo, Oslo, 2001.

[24] K.H. Esbensen, P. Geladi, Principles of Proper Validation: use and abuse of re-sampling for validation, Journal of Chemometrics, 24 (2010) 168-187.

[25] I.B. Haugland, J. Chladek, M. Halstensen, A feasibility study of real-time monitoring techniques for scale deposition thickness in pneumatic conveying pipelines, Particulate Science and Technology, 41 (2018) 1538-1543.